


Development of a long-acting direct-acting antiviral system for hepatitis C virus treatment in swine

Malvika Verma^{a,b,c,1}, Jacqueline N. Chu^{b,d,1}, John A. F. Salama^{b,1}, Mohammed T. Faiz^{b,1}, Feyisope Eweje^{b,e,f}, Declan Gwynne^{b,g}, Aaron Lopes^{b,g}, Kaitlyn Hess^{b,g}, Vance Soares^{b,g}, Christoph Steiger^{b,f,g}, Rebecca McManus^{b,g}, Ryan Koeppen^{b,e}, Tiffany Hua^{b,g}, Alison Hayward^{b,g,h}, Joy Collins^{b,g}, Siddhartha M. Tamang^{b,g}, Keiko Ishida^{b,g}, Jonathan B. Millerⁱ, Stephanie Katz^j, Alexander H. Slocum^{c,e}, Mark S. Sulkowski^j, David L. Thomas^j, Robert Langer^{a,b,c,e,g,2} , and Giovanni Traverso^{b,c,e,f,2}

^aDepartment of Biological Engineering, Massachusetts Institute of Technology, Cambridge, MA 02139; ^bKoch Institute for Integrative Cancer Research, Massachusetts Institute of Technology, Cambridge, MA 02139; ^cTata Center for Technology and Design, Massachusetts Institute of Technology, Cambridge, MA 02139; ^dDivision of Gastroenterology, Massachusetts General Hospital, Harvard Medical School, Boston, MA 02114; ^eDepartment of Mechanical Engineering, Massachusetts Institute of Technology, Cambridge, MA 02139; ^fDivision of Gastroenterology, Hepatology, and Endoscopy, Brigham and Women's Hospital, Harvard Medical School, Boston, MA 02115; ^gDepartment of Chemical Engineering, Massachusetts Institute of Technology, Cambridge, MA 02139; ^hDivision of Comparative Medicine, Massachusetts Institute of Technology, Cambridge, MA 02139; ⁱSloan School of Management, Massachusetts Institute of Technology, Cambridge, MA 02139; and ^jDivision of Infectious Diseases, Johns Hopkins University School of Medicine, Baltimore, MD 21205

Edited by Catherine J. Murphy, University of Illinois at Urbana-Champaign, Urbana, IL, and approved April 14, 2020 (received for review March 31, 2020)

Chronic hepatitis C virus (HCV) infection is a leading cause of cirrhosis worldwide and kills more Americans than 59 other infections, including HIV and tuberculosis, combined. While direct-acting antiviral (DAA) treatments are effective, limited uptake of therapy, particularly in high-risk groups, remains a substantial barrier to eliminating HCV. We developed a long-acting DAA system (LA-DAAS) capable of prolonged dosing and explored its cost-effectiveness. We designed a retrievable coil-shaped LA-DAAS compatible with nasogastric tube administration and the capacity to encapsulate and release gram levels of drugs while resident in the stomach. We formulated DAAs in drug-polymer pills and studied the release kinetics for 1 mo in vitro and in vivo in a swine model. The LA-DAAS was equipped with ethanol and temperature sensors linked via Bluetooth to a phone application to provide patient engagement. We then performed a cost-effectiveness analysis comparing LA-DAAS to DAA alone in various patient groups, including people who inject drugs. Tunable release kinetics of DAAs was enabled for 1 mo with drug-polymer pills in vitro, and the LA-DAAS safely and successfully provided at least month-long release of sofosbuvir in vivo. Temperature and alcohol sensors could interface with external sources for at least 1 mo. The LA-DAAS was cost-effective compared to DAA therapy alone in all groups considered (base case incremental cost-effectiveness ratio \$39,800). We believe that the LA-DAAS system can provide a cost-effective and patient-centric method for HCV treatment, including in high-risk populations who are currently undertreated.

Hepatitis C virus (HCV) infection is one of the main causes of chronic liver disease worldwide (1–3). One forecast predicted that mortality from chronic hepatitis would exceed the mortality caused by HIV, tuberculosis (TB), and malaria combined by 2040 (4). Accordingly, the World Health Organization has called for elimination of HCV infection by 2030 (5, 6).

Encouragingly, the development of direct-acting antiviral (DAA) therapy for HCV has revolutionized the field. The high cure rate of DAA therapies, with rates of sustained virologic response (SVR) of greater than 95%, short duration of treatment, and tolerability, has greatly expanded the number of patients being cured of chronic HCV (1, 2, 7, 8). However, due to factors such as cost, limited access to medical care, and inconsistent follow-up, less than half of those infected are actually treated (3, 8–10). People who inject drugs (PWID) have especially low HCV treatment uptake, despite being a large reservoir for chronic HCV infection (50% of all PWID globally) and the leading population infected with acute HCV (9, 11).

Particular challenges facing the PWID population include homelessness, which can make storage of oral medications difficult; comorbid psychiatric conditions; limited access to healthcare;

and distrust of the medical system (3). Modeling studies have suggested that expanding treatment to PWID can reduce transmission of HCV, even with poor rates of adherence and SVR (12). Studies utilizing methadone programs to deliver HCV treatment show promise, with high rates of treatment completion and SVR (3). However, such programs require significant infrastructure and cost and do not capture PWID who do not engage in other opioid agonist therapies such as buprenorphine or who may engage only intermittently (3, 13). Challenges that all populations face with regard to oral therapies include forgetfulness, low priority, pill phobia, dysphagia, and pill burden (14); rates of adherence to chronic medications in general are, at most, 50%, though higher

Significance

Direct-acting antiviral (DAA) therapy is highly effective against hepatitis C virus (HCV). Despite this, the burden of chronic HCV remains high, particularly in populations for whom daily medications can be challenging. The generation of long-acting modes of DAA delivery could thus expand HCV treatment. We have developed a long-acting DAA system (LA-DAAS) that can support multigram-level drug depots of HCV DAAs and provide controlled release of those drugs over the course of weeks. We demonstrate initial safety and efficacy of the LA-DAAS in a swine model. Expanding the range of delivery options of DAAs to patients and healthcare providers will further efforts toward global elimination of HCV infection.

Author contributions: M.V., J.N.C., J.A.F.S., M.T.F., A.H.S., M.S.S., D.L.T., R.L., and G.T. designed research; M.V., J.N.C., J.A.F.S., M.T.F., F.E., D.G., A.L., K.H., V.S., C.S., R.M., R.K., T.H., A.H., J.C., S.M.T., K.I., J.B.M., and S.K. performed research; R.L. contributed new reagents/analytic tools; M.V., J.N.C., J.A.F.S., M.T.F., F.E., and G.T. analyzed data; and M.V., J.N.C., R.L., and G.T. wrote the paper.

Competing interest statement: M.V., J.N.C., J.A.F.S., F.E., C.S., R.K., R.L., and G.T. are co-inventors on multiple patent applications describing gastric resident systems for extended drug release and intragastric sensing. R.L. and G.T. have a financial interest in Lyndra Therapeutics, Inc.; Suono Bio, Inc.; and Celero Systems, Inc., which are biotechnology companies focused on the development of gastrointestinal drug delivery and sensing technologies. Complete details for R.L. can be found at the following link: <https://www.dropbox.com/s/yc3xqb5s8s94v7x/Rev%20Langer%20COI.pdf?dl=0>. Complete details for G.T. can be found at the following link: <https://www.dropbox.com/s/shsz7vnr4a2ajb56/AABs5N5i0q9AfT1lqJAE-T5a?dl=0>. The remaining authors disclose no competing interests.

This article is a PNAS Direct Submission.

Published under the PNAS license.

¹M.V., J.N.C., J.A.F.S., and M.T.F. contributed equally to this work.

²To whom correspondence may be addressed. Email: rlanger@mit.edu or cgt20@mit.edu.

This article contains supporting information online at <https://www.pnas.org/lookup/suppl/doi:10.1073/pnas.2004746117/-DCSupplemental>.

First published May 18, 2020.

for short courses of therapy such as DAAs (14). Thus, there is a clear need for alternative strategies to deliver HCV treatment, and long-acting treatment delivery systems are one of the innovative strategies that have been endorsed, including recently by Unitaid (15, 16).

A long-acting DAA system (LA-DAAS) has the potential to safely and consistently deliver DAA therapy to patients with good adherence and quality of life by decreasing the frequency of dosing, with the goal of ultimately providing single dosing (14, 15). We have previously described a coil-shaped gastric resident system (GRS) which, due to its dimensions and mechanical properties, can remain resident in the gastric cavity and deliver multi-gram levels of drugs for TB, which has similar treatment challenges as HCV with frequent and daily dosing (17–19). Here, we describe the development of a LA-DAAS inspired by the multigram GRS with evaluation in a swine model of chronic HCV. We developed additional features, including integration of ethanol, temperature, and Bluetooth sensors, to enable patient engagement via wireless communication with the LA-DAAS. Such tools have improved

patient adherence to HCV therapy in other preliminary devices (20, 21). We then evaluated the cost-effectiveness of the LA-DAAS in general and PWID populations.

Results

Design of the LA-DAAS. The LA-DAAS design was inspired by a previous multigram GRS used for monthly treatment of TB (*SI Appendix*) (17). The LA-DAAS consists of drug-polymer pills strung along a superelastic nitinol wire (22). It can be administered via a nasogastric tube and forms a cylindrical coil upon reaching the stomach. During its residence in the gastric cavity, the LA-DAAS continually releases grams of drugs and is retrieved back through a nasogastric tube (Fig. 1 *A* and *B*). Electronic sensors were added to each end of the LA-DAAS to provide information on alcohol intake and body temperature, and to engage patients during their treatment. As alcohol use can cause further liver injury and accelerate disease progression, it is important for patients and clinicians to be aware of alcohol intake. However, patients may underestimate or underreport alcohol use due to

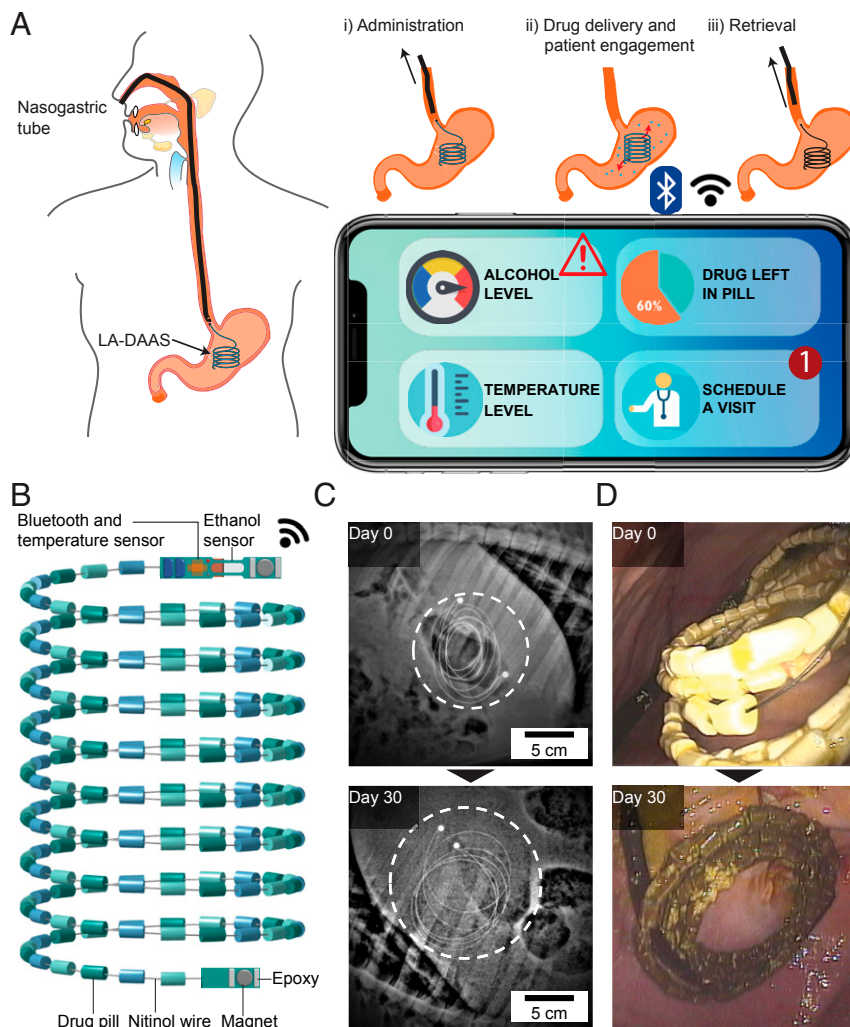


Fig. 1. Design and in vivo retention of the LA-DAAS. (*A, i*) A nasogastric (NG) tube is placed in a patient to administer the LA-DAAS, and then the NG tube is removed. (*A, ii*) The LA-DAAS resides in the gastric cavity while releasing DAAs. (*A, iii*) The NG tube is once again placed in a patient to deploy a retrieval device for attachment and removal of the LA-DAAS from the gastric cavity. The LA-DAAS is compatible with communication with a personal device, such as a smart phone, engaging patients to track alcohol and temperature levels and how much drug is left, and to schedule an appointment to receive another LA-DAAS. (*B*) The LA-DAAS consists of a series of drug pills on a coiled superelastic nitinol wire with end protected with epoxy and a magnet for retrieval. One end of the LA-DAAS is equipped with a Bluetooth, temperature, and alcohol sensor. (*C*) Representative radiographs of the LA-DAAS immediately after deployment and on day 30 in a swine model ($n = 3$). Dashed circles indicate location of the LA-DAAS. (*D*) Representative endoscopic images of the LA-DAAS immediately after deployment and on day 30 in a swine model ($n = 3$). For scale, each pill is 5 mm. Pentax endoscope magnification is up to 35 \times .

stigma, and physicians frequently fail to screen adequately for excessive alcohol intake (23, 24). An intragastric sensor can provide an objective measure of alcohol consumption and identify patients in need of therapy directed toward alcohol cessation (23). Additionally, patients with chronic liver disease—particularly PWID with chronic liver disease—are at higher risk of infection. To this end, a temperature sensor was also incorporated into the LA-DAAS in order to alert patients and physicians of fever or hypothermia that may signal a serious infection. Finally, patient engagement with treatment has been shown to improve adherence (20, 21, 25, 26). To this end, a Bluetooth and temperature sensor to confirm continual functional device status combined with a mobile software application was incorporated into the LA-DAAS. Messages could be sent to a patient's mobile device to remind them of clinic appointments or to return for repeat LA-DAAS administration and/or removal. In PWID or other high-risk populations where communication can be a challenge, a built-in device could improve outreach to patients. The physical dimensions of the LA-DAAS can be personalized to each patient, depending

on the target drug load and duration of therapy (*SI Appendix, Fig. S2*).

We evaluated month-long gastric retention of the LA-DAAS with Yorkshire swine, which have similar gastric anatomy to humans and have been used for evaluating previous long-acting drug delivery platforms (17, 27). Gastric residence of the LA-DAAS was confirmed for 30 d by using radiographs and endoscopy upon deployment and removal. Furthermore, the LA-DAAS remained in a coil shape. During the gastric residence period, the animals did not show any weight loss, evidence of obstruction, or limitation in passage of food or liquids; additionally, mucosal surfaces did not show injury, erosions, or ulcerations (*SI Appendix, Fig. S3*). Thus, we demonstrated the safe residence of the LA-DAAS in the gastric cavity for 1 mo.

In Vitro Release Kinetics of the LA-DAAS. We fabricated pills of model DAAs that we could procure mixed inside of a silicone or poly(ϵ -caprolactone) (PCL) matrix and spray-coated PCL coating around each pill to enable controlled release of the DAA

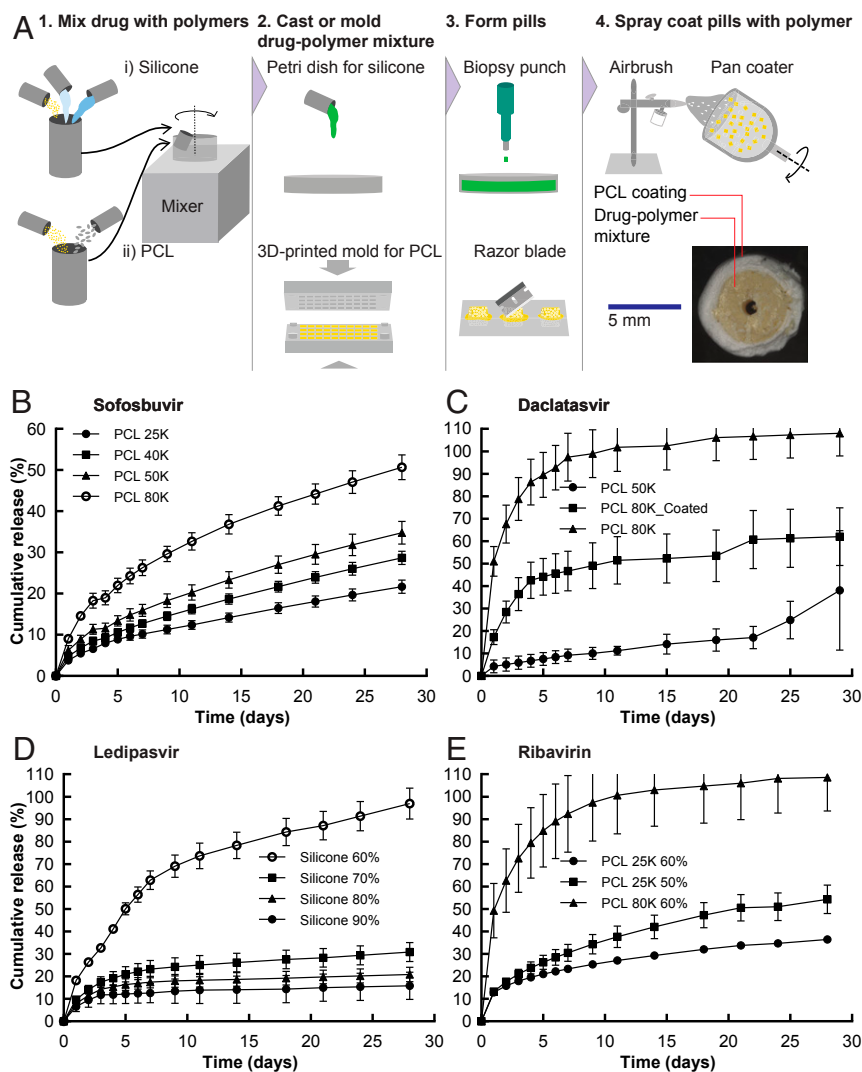


Fig. 2. Fabrication and in vitro release of DAAs from individual drug-polymer pills. (A) Drug-polymer pills are made by mixing drug with either silicone or PCL and then casting into a Petri dish or a three-dimensional (3D) printed mold. Drug-silicone pills are extracted by using a biopsy punch, and drug-PCL pills are extracted with a razor blade. Pills are then spray-coated with a pan coater. A cross-sectional image of a PCL-coated drug-PCL pill is shown. (B) In vitro release of sofosbuvir from a drug pill in water with varying molecular weights of PCL. (C) In vitro release of daclatasvir from a drug pill in water with varying molecular weights of PCL and PCL coating. (D) In vitro release of ledipasvir from a drug pill in acetonitrile with varying silicone hardness. (E) In vitro release of ribavirin from a drug pill in water with molecular weight of PCL and drug-loading percentage. Formulation compositions are available in *SI Appendix, Table S2*. Error bars represent SD for $n = 3$ samples.

(Fig. 24; $n = 3$ per formulation). Silicone and PCL have both been used as drug-release matrices for GRSs and have desirable mechanical properties for use in long-term drug delivery (17, 27, 28). Additionally, these polymers protect the DAA from degradation in acid. Within 7 d, sofosbuvir degrades by 95% in simulated gastric fluid (SGF) (*SI Appendix, Fig. S4*). However, when mixed with PCL, the drug-PCL pill shields the drug particles from degradation in acid (*SI Appendix, Fig. S5*). After submersion of drug-polymer pills in SGF for 3 d, PCL protected 89.75% of sofosbuvir, 82.39% of daclatasvir, and 87.11% of ribavirin. Silicone protected 98.96% of ledipasvir.

The DAA in powdered form was mixed homogeneously with either PCL or silicone to form a DAA-polymer blend, which was then casted or molded, followed by extraction of individual pills. During the mixing process of drug with PCL or silicone, the drug-polymer mixture was subjected to elevated temperatures. All four DAAs were stable after being subjected to 100 °C for 3 h, confirming that the manufacturing process did not affect drug stability (*SI Appendix, Fig. S6*). To prevent a burst release of drug, a layer of PCL was spray-coated on the surface of the pills (17, 28, 29). Each pill had a height and diameter of 5 mm with a 0.5-mm hole in the center through which to pass the nitinol wire and contribute to the assembled LA-DAAS.

We assembled drug-polymer pills for multiple DAAs, including sofosbuvir, daclatasvir, ledipasvir, and ribavirin (*SI Appendix, Table S2*) (30–34). Drug release occurred via diffusion through channels in the polymer matrix (17, 27, 35). Several factors contributed to tuning the drug-release rate from the polymer matrix, including the molecular weight of PCL, coating of the pill, the drug-loading percentage in the polymer matrix, and the surface-area-to-volume ratio of the pill (Fig. 2 B–E and *SI Appendix, Fig. S7*) (17, 28, 36–38). The rate of sofosbuvir release increased as the molecular weight of PCL increased from 25,000 to 80,000. More crystallinity (low amorphous regions) is associated with lower PCL molecular weight (38, 39). Therefore, the higher molecular weight has a faster degradation rate due to the presence of more amorphous regions. Increasing the surface-area-to-volume ratio of the pill also increased the sofosbuvir release rate. Daclatasvir release was modulated by varying the molecular weight of PCL and coating the pill to reduce the burst release of drug, resulting in a linear cumulative release versus time profile. Ribavirin release increased at higher PCL molecular weight and with a higher drug-loading percentage. Increasing the drug-loading percentage of ledipasvir resulted in a faster release rate. Overall, the drug-polymer pills provided a method to tune the release rate of four DAAs for 1 mo.

In Vivo Applications from the LA-DAAS. We next studied the long-term drug delivery of LA-DAAS in swine and evaluated its electronic-sensing capabilities. According to prior work we conducted in a swine model, the renally eliminated metabolite GS-331007 is the primary analyte of interest for clinical pharmacology studies with sofosbuvir (*SI Appendix, Fig. S8*) (40, 41). We prepared three LA-DAASs loaded with 11.2 g of sofosbuvir and administered them in swine. Each LA-DAAS was assembled to contain 300 pills using two different formulations, which released drug simultaneously (*SI Appendix, Table S3*). The serum concentration profile of a 400-mg single dose is shown in Fig. 3A. The drug was absorbed rapidly, and detectable concentrations were observed within 3 h. No drug was detectable after 1 d with the single-dose formulation. In contrast, drug was detectable for at least 28 d when sofosbuvir was dosed in the LA-DAAS (Fig. 3B). A 22.4-g LA-DAAS showed ongoing high levels of sofosbuvir release on day 30, suggestive of greater than 1-mo drug delivery capability (*SI Appendix, Table S4 and Fig. S9*).

After 1 mo of gastric residence in vivo, the LA-DAAS was retrieved, and the amount of sofosbuvir remaining in the pills was studied (*SI Appendix, Fig. S10*). The sofosbuvir-PCL pills

were completely dissolved, and the amount of sofosbuvir was quantified by using high-performance liquid chromatography (HPLC). These pills contained 15 to 50% of the initial sofosbuvir drug load prior to dosing in vivo. The addition of excipients, such as Pluronic P407 or poly(ethylene glycol), to the drug-PCL matrix increased the release rate of sofosbuvir (*SI Appendix, Fig. S11*) (28).

The LA-DAAS was equipped with a temperature sensor linked via Bluetooth to a phone application, as well as an alcohol sensor transmitting analog data to an external microcontroller. Batteries were included at the end of the LA-DAAS to provide power to the sensors (Fig. 3C). Prior to evaluation in a swine model, the sensors were studied for 1 mo in vitro immersed in SGF. The ethanol, temperature, and Bluetooth modules were insulated within a piece of tubing to shield them from gastric conditions. The head of the ethanol sensor was wrapped in a membrane for additional protection, and we successfully demonstrated the sensor's ability to respond to addition of ethanol at designated timepoints (*SI Appendix, Fig. S12*). The received signal-strength indication (RSSI) had an approximately linear relationship with distance between the Bluetooth transmitter and receiver, within 1 m of separation (*SI Appendix, Fig. S13*). Results indicated the stability of the Bluetooth module and temperature-sensor attachment during month-long exposure to acidic conditions (*SI Appendix, Fig. S14*). When evaluated in a euthanized swine's stomach, all sensors functioned as predicted—the ethanol sensor detected the addition of ethanol to gastric fluid, and the temperature sensor recorded the body temperature of the swine. A cell phone was able to receive the Bluetooth signal within 1 m.

Cost-Effectiveness of the LA-DAAS for HCV Treatment. We simulated two treatment strategies for patients: 1) standard DAA therapy or 2) the LA-DAAS (Fig. 4 A and B). In the base-case analysis of the LA-DAAS delivered nasogastrically once a month in patients with average adherence and likelihood of returning for repeat treatment, the LA-DAAS was cost-effective with an incremental cost-effectiveness ratio (ICER) of \$39,800 per quality-adjusted life-year (QALY) compared to conventional DAA therapy (Fig. 4C). We found that 96.7% of patients achieved SVR with the LA-DAAS compared to 93.9% with DAA therapy. The LA-DAAS was similarly cost-effective in PWID, with an ICER of \$36,700 per QALY. With the LA-DAAS, 96.3% of patients achieved SVR, compared to 90.5% with DAA therapy. Interestingly, the LA-DAAS was even more cost-effective when compared to a directly observed therapy (DOT) system, with an ICER of \$26,300 per QALY. We found that 96.3% of patients with the LA-DAAS achieved SVR compared to 92.6% with DOT.

One-way deterministic sensitivity analyses were performed to investigate the effects of changes in model parameters on estimated outcomes (*SI Appendix, Fig. S15*). Variables that changed the optimal strategy in the base case were disutility of LA-DAAS administration, cost of the LA-DAAS device, cost of LA-DAAS administration, treatment time course, and likelihood of not returning for repeat LA-DAAS administration. DAA became the preferred strategy if the LA-DAAS administration was particularly uncomfortable (disutility greater than -0.03 per administration, with 0 being no effect and -1 the equivalent of death) or if the cost of each administration were greater than \$2,700. The LA-DAAS remained cost-effective up to a device cost of \$3,700, which is comparable to the cost of intragastric balloons and other similar devices (*SI Appendix, Fig. S16A*) (42). The LA-DAAS remained cost-effective for HCV treatment courses of at least 5 wk, which represents the duration of all current HCV regimens (*SI Appendix, Fig. S16B*) (43). Finally, DAA became the preferred strategy if patients were unlikely to return for repeat LA-DAAS administration (probability of returning for repeat treatment only 30% over 1 y). Notable variables that

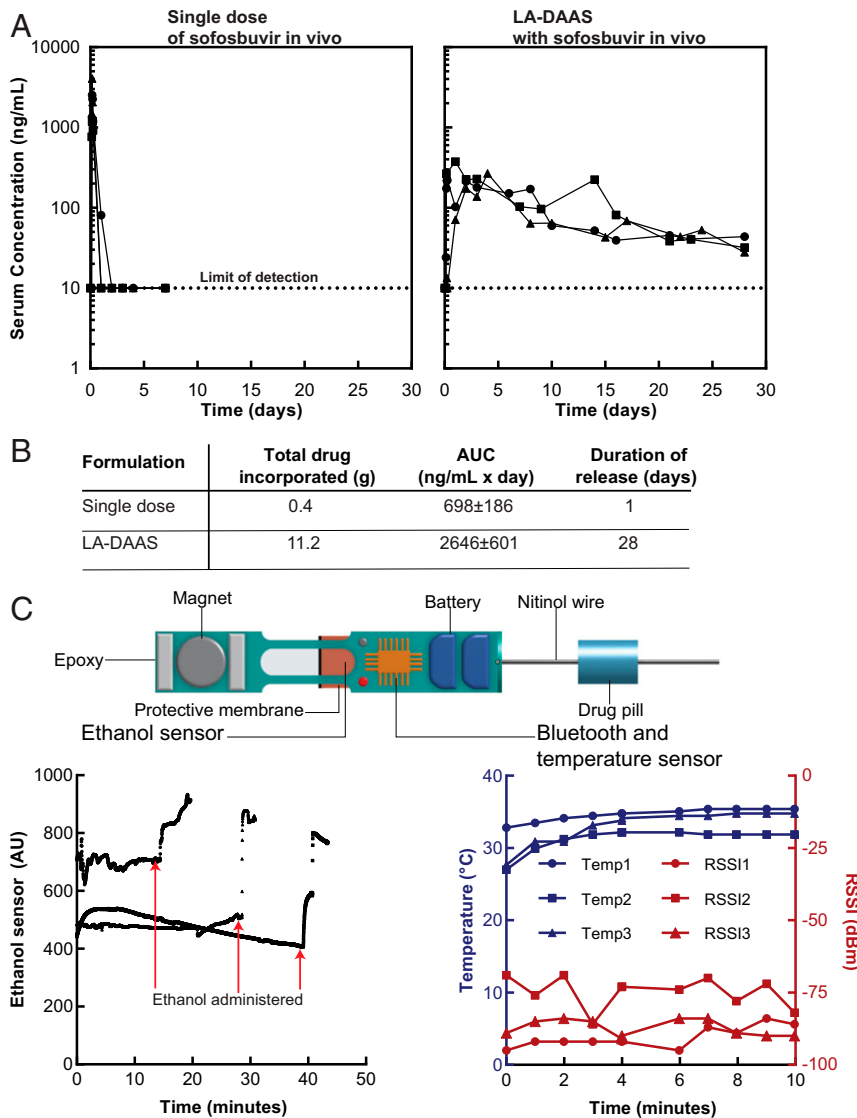


Fig. 3. In vivo applications of the LA-DAAS. (A, Left) Concentration-time profiles of the sofosbuvir metabolite GS-331007 in serum after administering a single dose of 400 mg ($n = 3$). (A, Right) Concentration-time profiles of the sofosbuvir metabolite GS-331007 in serum after administering the LA-DAAS, which had 11.2 g of sofosbuvir across two formulations ($n = 3$; *SI Appendix, Fig. S11*). (B) Area under the curve (AUC) and the duration of drug release for a single dose compared to the LA-DAAS administered in vivo, with the mean value and SD reported for $n = 3$ samples in each group. (C) Evaluation of the LA-DAAS electronic sensors ($n = 3$) in euthanized swine. The analog signal of the ethanol sensor, temperature, and RSSI were measured after placement of the LA-DAAS in the stomach. Ethanol was administered at the time indicated by the red point. Temperature levels are shown in blue, with the corresponding RSSI signal shown in red for the same LA-DAAS. AU, arbitrary units.

did not change the preferred treatment strategy included administration frequency of the LA-DAAS (dosing every 2, 4, 6, or 8 wk were all cost-effective) and age at beginning of treatment. We also performed a secondary analysis for single administration of the LA-DAAS, anticipating a future design capable of delivering a full treatment course, which found similar results (*SI Appendix, Table S5*). Overall, these results suggest that the LA-DAAS is cost-effective across many treatment and patient variables.

Discussion

With the development of effective and well-tolerated DAA therapy, it is now possible to cure hepatitis C in all patients. In this study, we describe a drug delivery system that can safely and effectively provide at least month-long doses of DAA therapy for HCV. Long-acting approaches to the treatment of HIV and TB

have been previously developed, and here we describe a long-acting enteral solution to the challenge of expanding HCV treatment (17, 44, 45). These data provide a basis for expanded research to adapt the technology to treatment of HCV-infected humans, including improving the system to ultimately achieve single-dose administration of HCV treatment.

Treatment of HCV infection historically involved the use of a pegylated form of interferon (IFN) alfa that prolonged half-life and allowed weekly dosing. An albumin-conjugated form of IFN with an even longer half-life was also considered (46). However, since the advent of DAA formulations, all treatment requires daily oral administration. We have now developed a long-acting enteral solution to enable monthly HCV treatment.

We anticipate that further development of the LA-DAAS will include further preclinical evaluation in additional animal models. Optimizing release kinetics from the drug-polymer pills

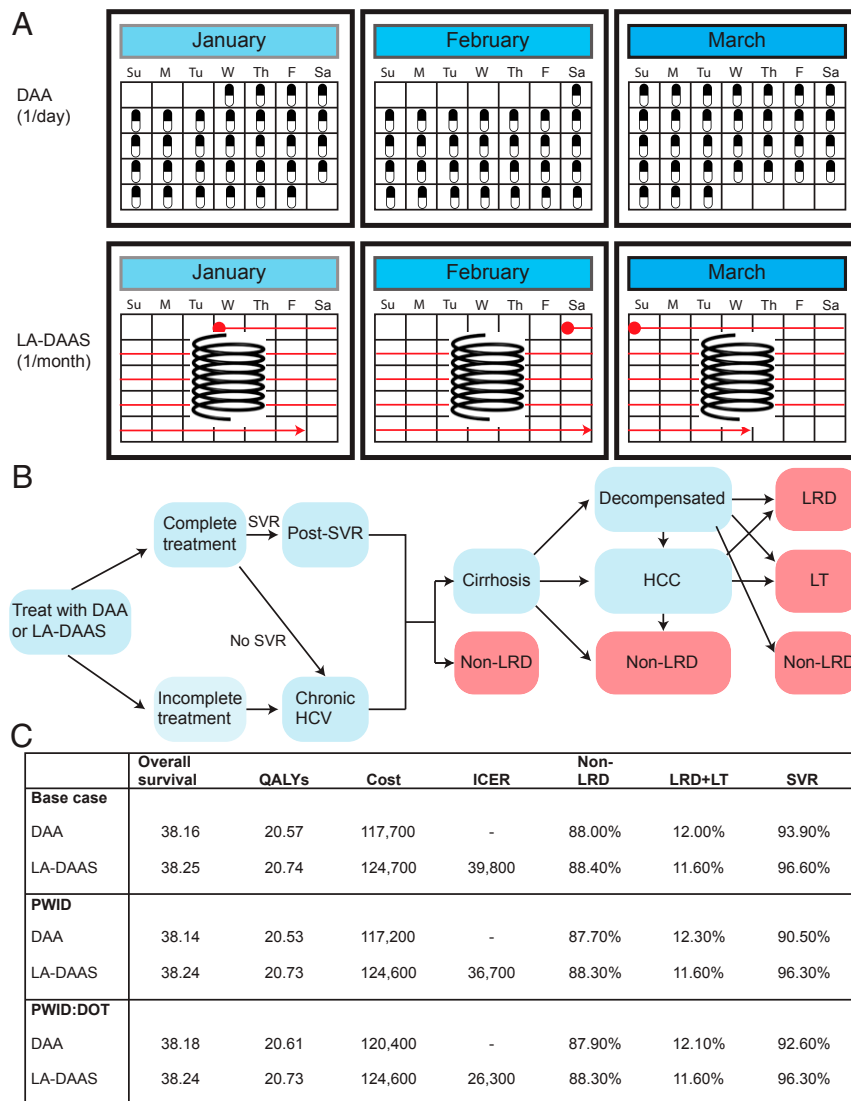


Fig. 4. Monthly HCV treatment and cost-effectiveness of a LA-DAAS. (A) Illustration of two treatment strategies for HCV treatment: Current HCV treatment spans 12 wk and involves daily administration of DAAs. The LA-DAAS can be administered once per month for HCV treatment. (B) Schematic of the cost-effectiveness model for chronic HCV with two treatment strategies, DAA or LA-DAAS. Transition states are shown in blue. Health states in red indicate death states or liver transplant, after which patients exit the model. HCC, hepatocellular carcinoma; LRD, liver-related death; LT, liver transplant; non-LRD, non-liver-related death. Table of parameters can be found in *SI Appendix, Table S1*. (C) Results for the cost-effectiveness analysis of DAA versus LA-DAAS. Results for three cohorts are presented. In the base case, patients treated have average adherence to DAA and average likelihood of returning for NGT retreatment. In the PWID case, patients have lower adherence than the general population and are less likely to return for repeated NGT treatment. In the PWID:DOT case, patients in the DAA arm are PWID treated in a DOT program. Cost and ICER are in US dollars. In all cohorts, treatment with LA-DAAS was cost-effective.

is a critical next step, such that serum concentrations of the drug remain within the therapeutic window for efficacious treatment with maximal release from the pills. We will also want to more closely mimic the typical regimens used in humans, including pangenotypic DAA formulations such as glecaprevir/pibrentasvir and study of daclatasvir or velpatasvir with sofosbuvir. Furthermore, based on our current data, future evaluation of prolonged gastric residency (>1 mo) and single administration of pangenotypic drug combinations is warranted. Additionally, long-term safety and stability of the electronic sensors must be assessed in the gastric environment, as well as long-term presence of the LA-DAA, for anticipated retrieval failure. Other considerations include whether nasogastric delivery of the LA-DAAS may be a challenge; although inexpensive, patients may find this delivery system uncomfortable. In such cases, endoscopic delivery may be

preferable and would also allow for greater volume of drug delivery and reduced dosing frequency.

Our economic analysis found that the LA-DAAS can be cost-effective across various patient populations, including both the general population and PWID. Although the LA-DAAS was generally preferred over DAA therapy in most scenarios tested, we identified several factors that could make conventional DAA therapy preferable to LA-DAAS: patients who find nasogastric delivery very unpleasant; high cost of the LA-DAAS or of its administration; short DAA treatment courses; and patients unlikely to return monthly for repeat LA-DAAS administration. This latter limitation could be particularly challenging in some settings. In others, such as in the correctional system, the LA-DAAS might be preferred over DAA therapy. For patients for whom nasogastric delivery is markedly unpleasant, one

could consider administration under sedation or endoscopically, although these costs were not analyzed in this model. Other populations that could benefit from this system include intubated and ventilated patients, such as posttransplant patients in the advent of HCV+ organ transplantation, particularly those requiring DAAs such as glecaprevir/pibrentasvir that cannot be crushed and administered through typical enteral access.

There are a number of limitations to our cost-effectiveness study. As with any modeling analysis, the accuracy of our model was restricted by available data. In particular, adherence rates, the impact of adherence on SVR, and the likelihood of returning for a repeated LA-DAAS administration were challenging to estimate. Therefore, we performed wide sensitivity analyses for these parameters. Our model did not capture the utility of reduced HCV transmission among PWID, which likely underestimates the overall benefit and cost-effectiveness of the LA-DAAS (11). Additionally, we did not include probability of reinfection in our model. If patients in one of the treatment strategies were reinfected more often than those in the other strategy, that would likely increase overall treatment costs in that arm and affect our calculated ICER. However, we do not expect that this would differ significantly between patients treated with DAA therapy versus the LA-DAAS. Finally, our model used the same drug cost for conventional DAA therapy and the cost of DAA included within the LA-DAAS (separate from device and administration costs). This assumes that further lowering of drug cost for DAAs will be applicable to the LA-DAAS as well. If there are heavy discounts applied to oral DAA therapy that are not included in pricing of the LA-DAAS, then the LA-DAAS could become cost-ineffective.

Ultimately, whether any given patient is more likely to adhere to or prefer daily pills versus monthly repeated nasogastric treatment will vary depending on the patient, and patient preference regarding modality of HCV treatment should guide choice of therapy. Further steps in development of the LA-DAAS should include engaging patients and healthcare providers in the hepatitis C community to evaluate the acceptability and feasibility of such an approach, as well as ongoing work to move toward single-dose administration for full HCV treatment. We believe that providing a range of delivery options to patients and healthcare providers will aid in maximizing deployment of recognized effective DAAs.

Materials and Methods

LA-DAAS Prototyping and In Vitro Drug Release. LA-DAASs were assembled and in vitro drug release was evaluated by HPLC as described, with modifications including formulations for DAAs (*SI Appendix, Fig. S1*) (17). The following drugs were acquired: sofosbuvir (Hefei Hirusun Pharmatech Co., Ltd.), daclatasvir and ledipasvir (Hangzhou APiChem Technology Co, Ltd.), and ribavirin (ChemShuttle). Drug was mixed with either vinylpolysiloxane (Zhermack SpA) or PCL (Nexeo Solutions Inc.) in a SpeedMixer DAC 150.1 VFX-K (FlackTek Inc.). Drug-loading percentages were determined relative to the final polymer mixture weight: sofosbuvir (50%), daclatasvir (40%), ledipasvir (40%), and ribavirin (40%). Individual drug-polymer pills were used to evaluate long-term release kinetics ($n = 3$ per formulation). Pill formulations were incubated in a New Brunswick Innova 44 shaking incubator (Eppendorf) at 37 °C and 200 rpm in 50 mL of fluid for 28 d, with solution exchanges at specified time intervals. Drug concentrations were then analyzed by using an Agilent 1260 Infinity II HPLC system.

In Vivo Evaluation of the LA-DAAS. All animal experiments were performed in accordance with protocols approved by the Committee on Animal Care at the Massachusetts Institute of Technology as described (17). To assess the oral pharmacokinetics of immediate release formulations and the LA-DAAS, we administered them to female 30- to 75-kg Yorkshire swine ($n = 3$ per formulation). Animals were fed daily in the morning and in the evening with a diet consisting of pellets (Laboratory Minipig Grower Diet, catalog no. 5081), in addition to a midday snack consisting of various fruits and vegetables. The

immediate release formulation was prepared by weighing and filling 400 mg of sofosbuvir in two "00" gelatin capsules 15 min prior to dosing. Prior to dosing, the swine were sedated with Telazol (5 mg/kg intramuscular [IM]), xylazine (2 mg/kg IM), and atropine (0.04 mg/kg IM); intubated; and maintained with isoflurane (1 to 3% inhaled). Immediate-release formulations and the LA-DAAS were deployed in the stomach via an endoscopic guided overtube. The overtube was removed after the devices were administered. For evaluation of the safety and residence time of the LA-DAAS, the animals were clinically assessed twice a day for evidence of gastrointestinal (GI) obstruction, including inappetence, abdominal distension, lack of stool, and vomiting. Additionally, the animals were evaluated radiographically every 3 to 4 d for evidence of GI obstruction and/or perforation. Tissue samples were collected before and after the device was placed in the stomach for histopathological analysis, and macroscopic images were taken once the device was retrieved to study any possible mucosal damage. At indicated time points, blood samples (3 mL) were collected from a central venous catheter. Serum samples were separated from blood by centrifugation (3,220 rpm; 10 min at 4 °C) and were stored at -80 °C for further analysis. Drug concentrations in serum were analyzed by using ultra-performance liquid chromatography (UPLC)-tandem mass spectrometry on a Waters ACQUITY UPLC-I-Class System aligned with a Waters Xevo-TQ-S mass spectrometer (Waters Corp.).

Integration and Evaluation of Electronic Sensors. The MQ3 alcohol sensor and required accessories were purchased from Digi-Key. The sensor was encapsulated in a 0.5- μ m pore polytetrafluorethylene membrane (Cole-Parmer) attached to one end of the LA-DAAS in Tygon tubing and connected to an Arduino Uno microcontroller (Digi-Key) to output the sensor reading. The other end of the LA-DAAS consisted of a TMP36 analog temperature sensor (Analog Devices, Inc.) soldered to an Adafruit Feather 32u4 Bluefruit (Adafruit Industries), a breakout board for the ATmega32u4 microcontroller (Atmel Corporation) and the nRF51822 BLE system (Nordic Semiconductor). Temperature and elapsed time since administration data were delivered to an iOS-enabled mobile phone (Apple Inc.) via an application with a user interface. Long-term stability of the sensors attached to the LA-DAAS were evaluated for 28 d in SGF. Ex vivo evaluation was conducted in euthanized swine to measure ethanol and temperature in gastric fluid as well as the RSSI.

Cost-Effectiveness Model Design. A Markov model of patients treated with either standard DAA therapy or with the LA-DAAS (dosed monthly) was constructed in TreeAge Pro. Model parameters were estimated from the literature and prior published models of HCV (*SI Appendix, Table S1*) (11, 47, 48). The simulated cohort of 40-y-old noncirrhotic men was followed over a lifetime time horizon. Three main cohorts were simulated: a base-case cohort with average DAA adherence and likelihood of returning for repeat LA-DAAS administration; a cohort of PWID with lower adherence and likelihood of returning; and a cohort of PWID enrolled in a DOT program with improved DAA adherence, but lower likelihood of returning for repeat LA-DAAS. After treatment with DAA or LA-DAAS for 12 wk, patients in each cohort would either complete treatment or not (depending on adherence and likelihood of returning for repeat LA-DAAS) and then either achieve SVR or continue with chronic HCV. Patients could then progress to cirrhosis and then to decompensation, HCC, liver-related death, or liver transplant. All patients in the model could die of non-liver-related death. The Markov cycle length was 1 wk. The weekly cost of DAA therapy was estimated from wholesale cost estimates of glecaprevir/pibrentasvir, discounted by 50% to reflect current real-world costs (11). The cost of the LA-DAAS included cost of DAA therapy plus monthly device cost and nasogastric administration costs. The primary outcomes of the analysis were unadjusted life-years (overall survival), QALYs, and ICER per QALY between competing treatment strategies from a healthcare perspective. The willingness-to-pay threshold was \$100,000/QALY (49). Cost estimates were converted to 2019 US dollars using the Consumer Price Index (50). Future costs and QALYs were discounted by 3% annually. One-way sensitivity analyses were performed for all variables using ranges published in the literature. We also generated a secondary model evaluating single dosing of the LA-DAAS to test future versions of the device that we anticipate will be able to deliver a full course of HCV treatment.

Data Availability. All data are included in the manuscript and *SI Appendix*.

ACKNOWLEDGMENTS. This work was supported in part by a Massachusetts Institute of Technology (MIT) Tata Center Grant (to R.L. and G.T.); NIH Grant EB000244 (to R.L. and G.T.); and startup support from the MIT

Department of Mechanical Engineering (G.T.). M.V. was supported in part by the MIT Tata Center Grant and an NSF Graduate Research Fellowship. J.N.C. was supported by NIH Training Grant 5T32DK007191-45. C.S.

was supported in part by the Alexander von Humboldt Foundation. D.L.T. was supported by a supplement to Center for AIDS Research Grant 1P30AI094189.

1. S. Saab, L. Le, S. Saggi, V. Sundaram, M. J. Tong, Toward the elimination of hepatitis C in the United States. *Hepatology* **67**, 2449–2459 (2018).
2. O. Falade-Nwulia *et al.*, Oral direct-acting agent therapy for hepatitis C virus infection: A systematic review. *Ann. Intern. Med.* **166**, 637–648 (2017).
3. M. J. Akiyama *et al.*, Intensive models of hepatitis C care for people who inject drugs receiving opioid agonist therapy: A randomized controlled trial. *Ann. Intern. Med.* **170**, 594–603 (2019).
4. K. J. Foreman *et al.*, Forecasting life expectancy, years of life lost, and all-cause and cause-specific mortality for 250 causes of death: Reference and alternative scenarios for 2016–40 for 195 countries and territories. *Lancet* **392**, 2052–2090 (2018).
5. World Health Organization, “Global hepatitis report, 2017” (WHO Rep., World Health Organization, Geneva, Switzerland, 2017).
6. D. L. Thomas, Global elimination of chronic hepatitis. *N. Engl. J. Med.* **380**, 2041–2050 (2019).
7. A. S. Lok *et al.*, Benefits of direct-acting antivirals for hepatitis C. *Ann. Intern. Med.* **167**, 812–813 (2017).
8. S. Barua *et al.*, Restrictions for Medicaid reimbursement of sofosbuvir for the treatment of hepatitis C virus infection in the United States. *Ann. Intern. Med.* **163**, 215–223 (2015).
9. J. Grebely, B. Hajarizadeh, G. J. Dore, Direct-acting antiviral agents for HCV infection affecting people who inject drugs. *Nat. Rev. Gastroenterol. Hepatol.* **14**, 641–651 (2017).
10. G. S. Cooke *et al.*; Lancet Gastroenterology & Hepatology Commissioners, Accelerating the elimination of viral hepatitis: A Lancet Gastroenterology & Hepatology Commission. *Lancet Gastroenterol. Hepatol.* **4**, 135–184 (2019).
11. E. D. Bethea, Q. Chen, C. Hur, R. T. Chung, J. Chhatwal, Should we treat acute hepatitis C? A decision and cost-effectiveness analysis. *Hepatology* **67**, 837–846 (2018).
12. N. K. Martin *et al.*, Hepatitis C virus treatment for prevention among people who inject drugs: Modeling treatment scale-up in the age of direct-acting antivirals. *Hepatology* **58**, 1598–1609 (2013).
13. J. W. Ward, A. R. Hinman, What is needed to eliminate hepatitis B virus and hepatitis C virus as global health threats. *Gastroenterology* **156**, 297–310 (2019).
14. L. Osterberg, T. Blaschke, Adherence to medication. *N. Engl. J. Med.* **353**, 487–497 (2005).
15. C. Flexner, D. L. Thomas, S. Swindells, Creating demand for long-acting formulations for the treatment and prevention of HIV, tuberculosis, and viral hepatitis. *Curr. Opin. HIV AIDS* **14**, 13–20 (2019).
16. Unitaid, “Impact story: Paving the way to hepatitis C elimination” (Tech. Rep., Unitaid, Geneva, Switzerland, 2018).
17. M. Verma *et al.*, A gastric resident drug delivery system for prolonged gram-level dosing of tuberculosis treatment. *Sci. Transl. Med.* **11**, 1–8 (2019).
18. M. Verma, J. Furin, R. Langer, G. Traverso, Making the case: Developing innovative adherence solutions for the treatment of tuberculosis. *BMJ Glob. Health* **4**, e001323 (2019).
19. World Health Organization, “Guidelines for the care and treatment of persons diagnosed with chronic hepatitis C virus infection” (Tech. Rep., World Health Organization, Geneva, Switzerland, 2018).
20. X. Wang, M. Bonacini, K. Liu, W. C. Lee, The impact of digital medicine program on economic and public health benefits for HCV coverage expansion from a state Medicaid perspective. *Value Health* **22** (suppl. 2), S201 (2019).
21. ClinicalTrials.gov, Digimeds to optimize adherence in patients with hepatitis C and increased risk for nonadherence (DASH). <https://clinicaltrials.gov/ct2/show/NCT03164902>. Accessed 8 July 2019.
22. T. Duerig, A. Pelton, D. Stöckel, An overview of nitinol medical applications. *Mater. Sci. Eng. A* **273–275**, 149–160 (1999).
23. R. S. O’Shea, S. Dasarthy, A. J. McCullough; Practice Guideline Committee of the American Association for the Study of Liver Diseases; Practice Parameters Committee of the American College of Gastroenterology, Alcoholic liver disease. *Hepatology* **51**, 307–328 (2010).
24. K. M. Ward *et al.*, A randomized controlled trial of cash incentives or peer support to increase HCV treatment for persons with HIV who use drugs: The CHAMPS study. *Open Forum Infect. Dis.* **6**, ofz166 (2019).
25. World Health Organization, “Patient engagement” (Technical Series on Safer Primary Care, World Health Organization, Geneva, Switzerland, 2016).
26. Y. L. Kong *et al.*, 3D-printed gastric resident electronics. *Adv. Mater. Technol.* **4**, 1800490 (2019).
27. A. M. Bellinger *et al.*, Oral, ultra-long-lasting drug delivery: Application toward malaria elimination goals. *Sci. Transl. Med.* **8**, 365ra157 (2016).
28. R. Kanasty *et al.*, A pharmaceutical answer to nonadherence: Once weekly oral memantine for Alzheimer’s disease. *J. Control. Release* **303**, 34–41 (2019).
29. S. Bose, A. A. Vu, K. Emshadi, A. Bandyopadhyay, Effects of polycaprolactone on alendronate drug release from Mg-doped hydroxyapatite coating on titanium. *Mater. Sci. Eng. C* **88**, 166–171 (2018).
30. World Health Organization, “Progress report on access to hepatitis C treatment: Focus on overcoming barriers in low-and middle-income countries, March 2018” (Tech. Rep. WHO/CDS/HIV/18.4, World Health Organization, Geneva, Switzerland, 2018).
31. M. E. Tucker, FDA approves “game changer” hepatitis C drug sofosbuvir. *Medscape Medical News*, 7 June 2019. <https://www.medscape.com/viewarticle/817371>. Accessed 8 July 2019.
32. Hepatitis C Online, Ledipasvir-sofosbuvir (Harvoni). <https://www.hepatitis-c.uw.edu/page/treatment/drugs/ledipasvir-sofosbuvir>. Accessed 7 June 2019.
33. D. Gritsenko, G. Hughes, Ledipasvir/sofosbuvir (Harvoni): Improving options for hepatitis C virus infection. *P&T* **40**, 256–276 (2015).
34. D. R. Nelson *et al.*; ALLY-3 Study Team, All-oral 12-week treatment with daclatasvir plus sofosbuvir in patients with hepatitis C virus genotype 3 infection: ALLY-3 phase III study. *Hepatology* **61**, 1127–1135 (2015).
35. Y. Fu, W. J. Kao, Drug release kinetics and transport mechanisms from semi-interpenetrating networks of gelatin and poly(ethylene glycol) diacrylate. *Pharm. Res.* **26**, 2115–2124 (2009).
36. A. Goyanes, P. Robles Martinez, A. Buanz, A. W. Basit, S. Gaisford, Effect of geometry on drug release from 3D printed tablets. *Int. J. Pharm.* **494**, 657–663 (2015).
37. S. Babaei *et al.*, Temperature-responsive biometamaterials for gastrointestinal applications. *Sci. Transl. Med.* **11**, 1–13 (2019).
38. F. Tuba, L. Oláh, N. Nagy, Towards the understanding of the molecular weight dependence of essential work of fracture in semi-crystalline polymers: A study on poly(ϵ -caprolactone). *Express Polym. Lett.* **8**, 869–879 (2014).
39. L. A. Bosworth, S. Downes, Physicochemical characterisation of degrading polycaprolactone scaffolds. *Polym. Degrad. Stabil.* **95**, 2269–2276 (2010).
40. B. J. Kirby, W. T. Symonds, B. P. Kearney, A. A. Mathias, Pharmacokinetic, pharmacodynamic, and drug-interaction profile of the hepatitis C virus NS5B polymerase inhibitor sofosbuvir. *Clin. Pharmacokinet.* **54**, 677–690 (2015).
41. D. Babusis *et al.*, Sofosbuvir and ribavirin liver pharmacokinetics in patients infected with hepatitis C virus. *Antimicrob. Agents Chemother.* **62**, 1–11 (2018).
42. J. A. Quinlan, Gastric balloon cost, insurance & discounts. *Bariatric Surgery Source*. <https://www.bariatric-surgery-source.com/gastric-balloon-cost.html>. Accessed 4 April 2019.
43. AASLD-IDS, Recommendations for testing, managing, and treating hepatitis C. <https://www.hcvguidelines.org>. Accessed 31 May 2019.
44. A. R. Kirtane *et al.*, Development of an oral once-weekly drug delivery system for HIV antiretroviral therapy. *Nat. Commun.* **9**, 2 (2018).
45. G. van’t Klooster *et al.*, Pharmacokinetics and disposition of rilpivirine (TMC278) nanosuspension as a long-acting injectable antiretroviral formulation. *Antimicrob. Agents Chemother.* **54**, 2042–2050 (2010).
46. S. Zeuzem *et al.*, Albinterferon alfa-2b dosed every two or four weeks in interferon-naïve patients with genotype 1 chronic hepatitis C. *Hepatology* **48**, 407–417 (2008).
47. J. T. Stahmeyer, S. Rossol, S. Liersch, I. Guerra, C. Krauth, Cost-effectiveness of treating hepatitis C with sofosbuvir/ledipasvir in Germany. *PLoS One* **12**, e0169401 (2017).
48. R. San Miguel, V. Gimeno-Ballester, A. Blázquez, J. Mar, Cost-effectiveness analysis of sofosbuvir-based regimens for chronic hepatitis C. *Gut* **64**, 1277–1288 (2015).
49. P. J. Neumann, J. T. Cohen, M. C. Weinstein, Updating cost-effectiveness—the curious resilience of the \$50,000-per-QALY threshold. *N. Engl. J. Med.* **371**, 796–797 (2014).
50. Bureau of Labor Statistics, Consumer price index. <https://www.bls.gov/cpi/>. Accessed 12 March 2019.